

CeRh₃B₂: A ferromagnet with anomalously large Ce 5*d* spin and orbital magnetic moments

A. Yaouanc, P. Dalmas de Réotier, and J.-P. Sanchez

*Commissariat à l'Energie Atomique, Département de Recherche Fondamentale sur la Matière Condensée,
Service de Physique Statistique, Magnétisme et Supraconductivité, F-38054 Grenoble Cedex 9, France*

Th. Tschentscher

European Synchrotron Radiation Facility, Boîte Postale 220, F-38043 Grenoble Cedex 9, France

P. Lejay

*Centre de Recherches sur les Très Basses Températures, Centre National de la Recherche Scientifique,
Boîte Postale 166X, F-38042 Grenoble Cedex, France*

(Received 18 July 1997)

We report a high-energy magnetic-Compton-scattering study performed on the ferromagnet CeRh₃B₂. This technique solely measures the electron spin magnetic moments. In contrast to a number of Ce intermetallics with nonmagnetic elements, the Ce 5*d* spin moment is found to be large and parallel to the Ce 4*f* spin moment. Therefore the Kondo effect does not play a key role for CeRh₃B₂. The inferred large Ce 5*d* orbital magnetic moment is a signature of the strong spin-orbit interaction for the Ce 5*d* band. [S0163-1829(98)51502-0]

The ternary cerium boride CeRh₃B₂, which crystallizes in the hexagonal CeCo₃B₂ structure (space group *P6/mmm*), has attracted considerable interest due to its anomalous ferromagnetism. Its Curie temperature $T_C=115$ K is by far the highest Curie temperature of known Ce compounds with nonmagnetic constituents.¹ It is even beyond that of GdRh₃B₂ ($T_C=90$ K), in clear contrast to the de Gennes law prediction. Its saturation magnetization at low temperature is strongly reduced relative to the Ce³⁺ free ion value ($2.14\mu_B$). Using a superconducting-quantum-interference-device magnetometer we find $\mu_{\text{bulk}}=0.42\mu_B/\text{f.u.}$, in agreement with a recent determination,² but smaller than the $0.55\mu_B/\text{f.u.}$ previously reported.³ This magnetization lies within the *ab* plane. Photoemission spectroscopy,^{4,5} x-ray absorption spectroscopy⁶ as well as a La substitution study⁷ indicate that the Ce ions are in a trivalent state. According to a polarized neutron scattering study, the low temperature value of the total magnetic moment of the Ce 4*f* and 5*d* shells are, respectively, $\mu_{\text{Ce}}^T(4f)=0.56(3)\mu_B$ and $\mu_{\text{Ce}}^T(5d)=-0.18(2)\mu_B$.² This polarized neutron study confirms the trivalent state of Ce and shows that the total magnetic moment carried by the 4*d* electrons of Rh [$\mu_{\text{Rh}}^T(4d)$] and both the orbital and spin magnetic moments of the Rh 4*d* shell [$\mu_{\text{Rh}}^L(4d)$ and $\mu_{\text{Rh}}^S(4d)$, respectively] are negligible. Finally, we note that the sum of the Ce 4*f* and 5*d* moments $\mu_{\text{Ce}}^T(4f)+\mu_{\text{Ce}}^T(5d)\approx 0.38\mu_B$ is within the error bars very close to the bulk moment.

Several models have been proposed to explain the magnetic properties of CeRh₃B₂. They have been reviewed recently.⁸ Because the Ce 4*f* electrons are localized or nearly localized, a bandlike 4*f* model is inappropriate. While the anomalous ferromagnetism may originate from a strong hybridization between the Ce 4*f* and nearest-neighbor Ce 5*d* electrons, the Kondo effect on the Ce atom could be of importance as found in numerous Ce compounds. Since

$\mu_{\text{Ce}}^T(4f)$ is relatively large and both $\mu_{\text{Rh}}^S(4d)$ and $\mu_{\text{Rh}}^L(4d)$ are very small, the hybridization between the Ce 4*f* and the Rh 4*d* electrons is weak.

Recent years have seen a surge of activity in the use of photon beam techniques to study magnetic properties of materials.⁹ Among all the experimental techniques, magnetic x-ray diffraction, resonant Raman scattering, magnetic Compton scattering, and magnetic circular dichroism at absorption edges, the combination of the results of the latter two techniques offer the possibility to eventually determine the orbital ($\mu_L=-\langle L_z \rangle \mu_B$) and spin ($\mu_S=-2\langle S_z \rangle \mu_B$) magnetic moments of each electron shell for each ion species of a ferromagnet. The x-ray magnetic circular dichroism (XMCD) technique has already been used to measure $\mu_{\text{Ce}}^L(4f)$.⁶ The measurements seem to have been performed on a polycrystalline sample. If, using the value of $\mu_{\text{Ce}}^T(4f)$ measured by polarized neutron scattering, we renormalize the data of Ref. 6 to get the easy axis saturation value, we deduce $\mu_{\text{Ce}}^L(4f)=0.84\mu_B$ and $\mu_{\text{Ce}}^S(4f)=-0.28\mu_B$. However, we note that these values were obtained assuming $\mu_{\text{Ce}}^T(5d)=0.28\mu_B$ (renormalized value) at strong variance from the polarized neutron scattering result ($-0.18\mu_B$).

$\mu_{\text{Ce}}^T(5d)$ has been measured in a number of Ce compounds with nonmagnetic elements: CeSn₃, CeAl₂, CeSb, CeIn₃, and CeNi₂Al₅.¹⁰⁻¹² For all of them $\mu_{\text{Ce}}^T(5d)$ is positive. This property has been associated with the Kondo character of these compounds.¹¹ Interestingly, we note that the decomposition of $\mu_{\text{Ce}}^T(5d)$ in its orbital and spin components has never been determined for any Ce compound.

An independent measurement of $\mu_{\text{Ce}}^S(4f)$ and $\mu_{\text{Ce}}^S(5d)$ is therefore of great interest. Furthermore, these results in combination with the total moment of the Ce 4*f* and 5*d* shells as determined by neutron diffraction and bulk magnetization will allow for the separation of the spin and orbit contribution to these moments.

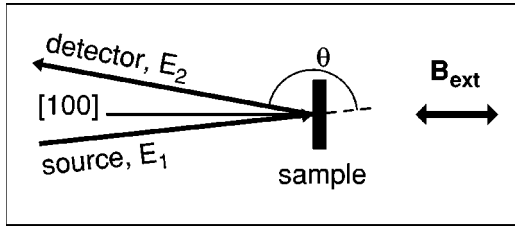


FIG. 1. The scattering geometry of the experiment: E_1 and E_2 are the energies of the incident and scattered photons, θ is the scattering angle ($\theta=171^\circ$). The sample was mounted in reflection geometry. An external magnetic field, \mathbf{B}_{ext} , of 0.92 T along the [100] crystallographic direction is applied alternatively parallel and antiparallel to the scattering vector for a duration of 50 s followed by a sleep time of 5 s.

In this paper we report an x-ray magnetic-Compton-scattering study carried out on a single crystal of CeRh_3B_2 . Magnetic Compton scattering has the advantage that only the distribution of the spin moments is measured, i.e., the technique is not sensitive to orbital moments. This is due to the very fast interaction of the photon with the scattered electron and has been first discovered experimentally¹³ and explained theoretically thereafter.^{14–16} If the electron density distributions of different electron states are sufficiently different, the partial magnetic spin moments can be determined. The magnetic-Compton-scattering cross section in the impulse approximation writes¹⁷

$$\left(\frac{d^2\sigma}{d\Omega dE_2}\right)_\epsilon = a(E_2)[J(p_z) + \epsilon b(E_2)J_{\text{mag}}(p_z)], \quad (1)$$

where the quantity ϵ is ± 1 depending on the direction of the external magnetic field \mathbf{B}_{ext} which is applied along the scattering vector chosen as the z direction. $a(E_2)$ and $b(E_2)$ are functions accounting for the experimental geometry. The two quantities of interest are the charge and magnetic Compton profiles denoted by $J(p_z)$ and $J_{\text{mag}}(p_z)$, respectively. p_z is the component of the ground state electron momentum along the z direction. $J(p_z)$ is the projection of the electron momentum density along z . $J_{\text{mag}}(p_z)$, the spin density distribution, is obtained from the difference in the total distribution when \mathbf{B}_{ext} is reversed (\uparrow to \downarrow), i.e.,

$$J_{\text{mag}}(p_z) = \int \int [n^\uparrow(\mathbf{p}) - n^\downarrow(\mathbf{p})] dp_x dp_y. \quad (2)$$

The measurements were performed at the European Synchrotron Radiation Facility (ESRF) using the end-station of the high energy beamline ID15A where best conditions for Compton scattering experiments can be achieved.¹⁸ The x-ray source was an asymmetric 7-pole wiggler with a critical energy of 45 keV providing circular polarized photons above and below the orbit plane. A horizontal reflecting single-bounce bent Si crystal was used as monochromator in Laue geometry. The (220) reflection was used and the crystal was bent to ≈ 60 m. The energy spectra were recorded for alternating \mathbf{B}_{ext} with an energy dispersive Ge-solid-state detector. Normalization of the incident flux was achieved by means of a Si-photodiode.

We used a standard backscattering geometry displayed in Fig. 1. A monochromatic beam of circular polarized syn-

chrotron radiation impinges on the sample which is placed in the magnetic field of a permanent magnet. Backscattering geometry is used to optimize the resolution due to geometrical broadening. The spin direction in the sample is flipped by turning the permanent magnet back and forth.

The experiments were performed with photons of energy $E_1=201$ keV. At this energy the resolution improves significantly to 0.40 a.u., compared to earlier magnetic Compton measurements done at an energy of ~ 60 keV, which had 0.70–0.75 a.u. resolution.¹⁹ In addition the magnetic contribution increases as one increases the incident photon energy. The magnetic Compton profile appears as an additional contribution to the scattering cross section around the charge Compton profile which is found for our geometry around 112 keV. Thus no disturbance from fluorescence lines at much lower energy is expected.

The sample was a single crystal coming from the same batch as the crystal measured recently in the neutron study.² It had a thickness ~ 1.5 mm and covered a surface of $\sim 6 \times 4$ mm². The x-ray beam probed only a surface of $\sim 3 \times 1$ mm². The data were recorded at 10 K. \mathbf{B}_{ext} was applied in the ab plane with $B_{\text{ext}}=0.92$ T. Under the present experimental conditions the bulk magnetization reaches its saturation value.

In comparison to earlier magnetic Compton measurements on CeFe_2 ,¹⁹ the measurements on CeRh_3B_2 are expected to be more difficult since an estimate shows that the magnetic signal should be four times smaller. This signal strength is determined by the ratio of the number of electrons carrying magnetic moment to the total number of electrons and by the overall spin magnetization. In our CeRh_3B_2 measurements the flipping ratio, which indicates the relative strength of the magnetic signal, was only 0.087(6)% compared to typically 2% for Fe at similar experimental conditions.²⁰ In addition the count rate is generally not limited by the x-ray source but the detector. This limitation can be overcome using a multielement detector. This is not presently available at ID15A.

In order to normalize the magnetic signal to an absolute magnetic moment, an auxiliary measurement was performed on Fe with the same experimental setup. We use the result $\int_{-8}^8 J_{\text{mag}}(p_z) dp_z = 2.07 \mu_B$.²¹ In Fe, the bulk magnetization, which is dominated by the 3d spin magnetic moment, aligns parallel to \mathbf{B}_{ext} . It is positive in our convention.

Following common practice (see Ref. 22), four corrections were made to the measured spectra. The data were corrected for the energy dependence of the cross section [proportional to $a(E_2)$], the absorption in the sample of the incoming and outgoing radiations, the detector efficiency and the effect of multiple scattering, which was studied by Monte Carlo simulation.²³ We found that $\sim 85\%$ of the scattering were single events, $\sim 13.5\%$ double events and $\sim 1.5\%$ triple events. The total amount of corrections applied to the total measured intensity for each direction was $\sim 14\%$. Because the magnetic signal is seen in the difference of spectra recorded for both field directions, the shape of the magnetic distribution does depend only very little on the corrections. On the opposite the total magnetic effect does depend on the corrections.

$J(p_z)$ can be deduced from the corrected spectra once they are put on an absolute scale. This was done with the help of the sum rule $\int_{-\infty}^{\infty} J(p_z) dp_z = Z_e$ where Z_e is the num-

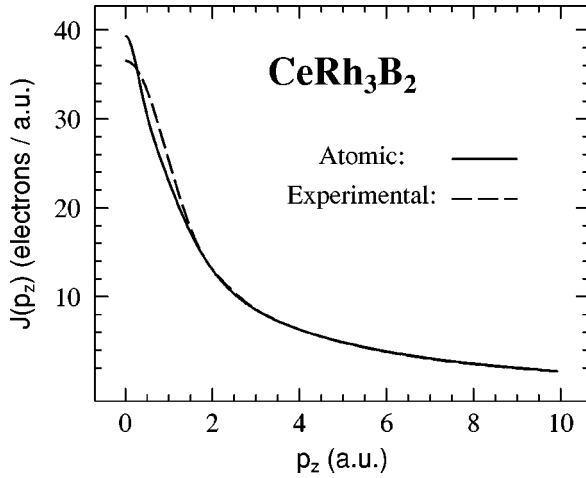


FIG. 2. Comparison between the measured and the atomic charge Compton profile of CeRh₃B₂. The large differences between the two profiles for $p_z < 2.0$ a.u. reflect solid state effects for the conduction electrons.

ber of electrons of the compound participating to the scattering. The integration was carried out for $|p_z| \leq 20$ a.u. and the normalization was done by comparison with the theoretical Compton profile computed using the relativistic calculations for atomlike profiles by Biggs *et al.*²⁴

In Fig. 2 the experimental and theoretical Compton charge profiles are compared in the range $|p_z| \leq 10$ a.u. The theoretical profile was convoluted with a Gaussian resolution function of 0.40 a.u. full width at half maximum. The experimental profiles for the two \mathbf{B}_{ext} directions cannot be distinguished in the scale of Fig. 2. We note the good agreement between the experimental and theoretical profiles for $p_z > 2.0$ a.u. reflecting that our systematic corrections, e.g., for absorption, detector efficiency, and multiple scattering, have been properly calculated. This indicates that we can rely on the region $p_z > 2.0$ a.u. of the magnetic Compton profile which is presented and analyzed in the following part of the text. The difference observed for $p_z < 2.0$ a.u. reflects the expected effects of the energy bands on the conduction electron momentum density. This comparison means that the atomic profile shapes are not reliable for conduction electrons with $p_z \leq 2.0$ a.u.

As indicated by Eq. (1), the difference between the corrected measured spectra with $\epsilon=1$ and $\epsilon=-1$ yields $2b(E_2)J_{\text{mag}}(p_z)$. $b(E_2)$ is the product of a function linear in energy and a constant which depends on the experimental geometry and is proportional to the degree of circular polarization of the x-ray beam. This prefactor was determined by the auxiliary measurement on Fe in comparison with its known spin magnetization.²¹ Thus we can establish an absolute scale for the magnetic Compton profile $J_{\text{mag}}(p_z)$ of CeRh₃B₂. We find for the total spin magnetic moment of CeRh₃B₂, $\mu_{\text{CeRh}_3\text{B}_2}^S = -0.79(6)\mu_B$. It is important to notice that the $\mu_{\text{CeRh}_3\text{B}_2}^S$ value is independent of the model used to describe the electrons (atomic or bandlike) and is relatively precise since it is the integral of the measured magnetic profile $[\int_{-\infty}^{\infty} J_{\text{mag}}(p_z) dp_z]$ normalized to the Fe experiment.

In Fig. 3 we present $J_{\text{mag}}(p_z)$ extracted from the measurements. Since $|J_{\text{mag}}(p_z)|$ decreases monotonically as p_z in-

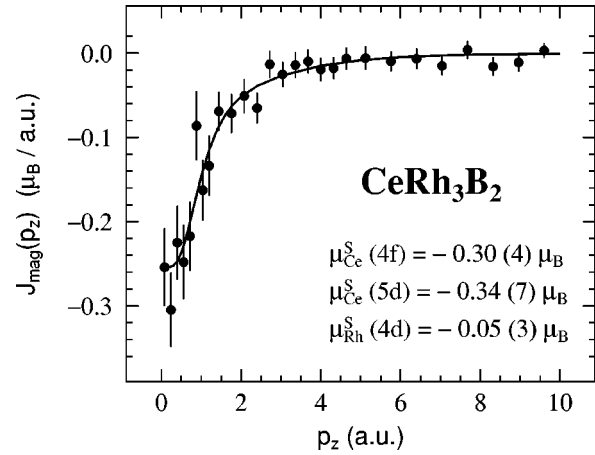


FIG. 3. Magnetic Compton profile of CeRh₃B₂ and best fit to the data. The obtained spin moment values are indicated in the figure. We have only taken into account data with $2 < p_z < 10$ a.u. for the fit.

creases, the three magnetic moments we are looking for are of the same sign, i.e., they are negative. We do not consider a possible contribution from the s and p conduction electrons by the Ce or Rh moments which in any case would be very small. In order to decompose $J_{\text{mag}}(p_z)$ we need to consider the relevant Compton profiles. They are presented in Fig. 4.

Contrary to the Ce $5d$ profile, the Ce $4f$ and Rh $4d$ profiles are p_z dependent for $p_z > 2.0$ a.u. As discussed above, in the high p_z regime the theoretical shapes can be trusted. Therefore it is possible from a fit to extract reliable values of $\mu_{\text{Ce}}^S(4f)$ and $\mu_{\text{Rh}}^S(4d)$. Then, since the total spin moment is known, the value of $\mu_{\text{Ce}}^S(5d)$ is safely determined from the relation $\mu_{\text{Ce}}^S(5d) = \mu_{\text{CeRh}_3\text{B}_2}^S - \mu_{\text{Ce}}^S(4f) - 3\mu_{\text{Rh}}^S(4d)$.

In Fig. 3 we present the best fit to the data (performed at momentum larger than 2 a.u.): it gives $\mu_{\text{Ce}}^S(4f) = -0.30(4)\mu_B$, $\mu_{\text{Ce}}^S(5d) = -0.34(7)\mu_B$, and $\mu_{\text{Rh}}^S(4d) = -0.05(3)\mu_B$. The Compton data are then consistent with the quasiabsence of spin moment on the Rh $4d$ electrons as found by neutron diffraction.

In order to test the quality of the information obtained from the analysis, we have tried other sets of parameters.

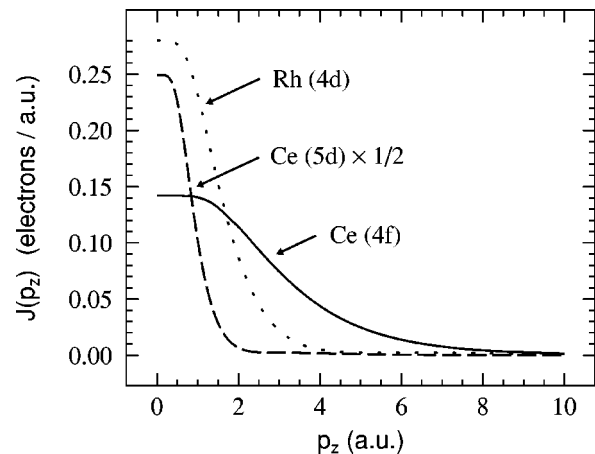


FIG. 4. Atomic Compton profiles of Rh $4d$, Ce $5d$, and Ce $4f$ (from Ref. 24). For Rh $4d$ we took the average value of the $4d^{(+)}$ and $4d^{(-)}$ profiles.

Setting the value $\mu_{\text{Ce}}^S(4f)$ for instance to $-0.2\mu_B$ gives reasonable fit to the data although not as good as the one presented in Fig. 3 but yields an unrealistic large value for $\mu_{\text{Rh}}^S(4d)$ ($-0.15\mu_B$) at odds from the neutron diffraction result. On the other hand setting $\mu_{\text{Ce}}^S(4f)$ to a value somewhat more negative than -0.30 definitively gives bad fits, especially in the region $3 \text{ a.u.} \leq p_z \leq 6 \text{ a.u.}$ The results of these two tests are qualitatively understood if one refers to Fig. 4.

From the value $\mu_{\text{Ce}}^T(4f)$ obtained from polarized neutron diffraction, we deduce that $\mu_{\text{Ce}}^L(4f) = 0.86(5)\mu_B$. Therefore the ratio $-\mu_{\text{Ce}}^L(4f)/\mu_{\text{Ce}}^S(4f) \approx 2.9$ clearly deviates from the value 4 expected from Hund's rule applied to the Ce^{3+} ion. A reduction of $-\mu_{\text{Ce}}^L(4f)/\mu_{\text{Ce}}^S(4f)$ compared to the free ion value is usually taken as a signature of hybridization.²⁵ Notice that due to the Wigner-Eckart theorem the ratio $-\mu_{\text{Ce}}^L(4f)/\mu_{\text{Ce}}^S(4f)$ is independent of the crystal field interaction as far as higher order multiplets are not involved. This assumption may not be justified for this compound since the mixing of the multiplets $J=5/2$ and $J=7/2$ could be important.⁸

In summary, the Compton measurements show that the Ce spin $5d$ moment is $-0.34(7)\mu_B$ and is antiparallel to $\mu_{\text{Ce}}^L(4f)$ meaning a ferromagnetic coupling between the $4f$ and $5d$ spins. Taking $\mu_{\text{Ce}}^T(5d) = -0.18(2)\mu_B$, we deduce $\mu_{\text{Ce}}^L(5d) = 0.16(7)\mu_B$. We have therefore obtained a value for the orbital moment of the rare-earth d band. Possible orbital polarization of the $5d$ band in rare-earth intermetallics has already been invoked in many instances.^{26,27} The sign of $\mu_{\text{Ce}}^S(5d)$ and $\mu_{\text{Ce}}^T(5d)$ is clearly at variance with expectation for Ce Kondo compounds.¹⁰⁻¹² Therefore the Kondo effect does not play a key role in the mechanism leading to the high T_C value. Since $\mu_{\text{Ce}}^L(5d)$ is rather large, strong spin-orbit interaction in the $5d$ band is expected.

It is a pleasure to acknowledge helpful discussions with P. Bonville, J. X. Boucherle, F. Givord, J. E. McCarthy, P. Suortti, and J. Schweizer. We thank V. Honkimaki for his help during the experiment and P. Fajardo for provision of the Monte Carlo code. The magnet was provided by the University of Warwick.

- ¹S. K. Dhar, S. K. Malik, and R. Vijayaraghavan, *J. Phys. C* **14**, L321 (1981).
- ²J. A. Alonso, J. X. Boucherle, F. Givord, J. Schweizer, B. Gillon, and P. Lejay, International Conference on Magnetism, Cairns, Australia, 1997 [*J. Magn. Magn. Mater.* (to be published)].
- ³M. Kasaya, A. Okabe, T. Takahashi, T. Satoh, T. Kasuya, and A. Fujimori, *J. Magn. Magn. Mater.* **76&77**, 347 (1988).
- ⁴E. V. Sampathkumaran, G. Kaindl, C. Laubschat, W. Krone, and G. Wortmann, *Phys. Rev. B* **31**, 3185 (1985).
- ⁵A. Fujimori, T. Takahashi, A. Okabe, M. Kasaya, and T. Kasuya, *Phys. Rev. B* **41**, 6783 (1990).
- ⁶J. Ph. Schillé, F. Bertran, M. Finazzi, Ch. Brouder, J. P. Kappler, and G. Krill, *Phys. Rev. B* **50**, 2985 (1994).
- ⁷S. A. Shaheen, J. S. Schilling, and R. N. Shelton, *Phys. Rev. B* **31**, 656 (1985).
- ⁸K. Yamaguchi, H. Namatame, F. Fujimori, T. Koide, T. Shidara, M. Nakamura, A. Misu, H. Fukutani, M. Yuri, M. Kasaya, H. Suzuki, and T. Kasuya, *Phys. Rev. B* **51**, 13 952 (1995).
- ⁹S. W. Lovesey and S. P. Collins, *X-Ray Scattering and Absorption by Magnetic Materials* (Clarendon Press, Oxford, 1996).
- ¹⁰C. Stassis, C.-K. Loong, B. N. Harmon, and S. H. Liu, *J. Appl. Phys.* **50**, 7567 (1979).
- ¹¹J. X. Boucherle and J. Schweizer, *Physica B* **130**, 337 (1985).
- ¹²J. X. Boucherle, F. Givord, J. Schweizer, and Y. Yshikawa, *Physica B* **234&236**, 875 (1997).
- ¹³M. J. Cooper, E. Zukowski, S. P. Collins, D. N. Timms, F. Itoh, and H. Sakurai, *J. Phys.: Condens. Matter* **4**, L399 (1992).
- ¹⁴N. Sakai, *J. Phys. Soc. Jpn.* **63**, 4655 (1994).
- ¹⁵S. W. Lovesey, *J. Phys.: Condens. Matter* **8**, L353 (1996).
- ¹⁶P. Carra, M. Fabrizio, G. Santoro, and B. T. Thole, *Phys. Rev. B* **53**, R5994 (1996).
- ¹⁷N. Sakai, *J. Appl. Crystallogr.* **29**, 81 (1996).
- ¹⁸P. Suortti and T. Tschentscher, *Rev. Sci. Instrum.* **66**, 1798 (1995).
- ¹⁹M. J. Cooper, P. K. Lawson, M. A. G. Dixon, E. Zukowski, D. N. Timms, F. Itoh, H. Sakurai, H. Kawata, Y. Tanaka, and M. Ito, *Phys. Rev. B* **54**, 4068 (1996).
- ²⁰J. E. McCarthy, M. J. Cooper, P. K. Lawson, D. N. Timms, S. O. Manninen, K. Hämäläinen, and P. Suortti, *J. Synchrotron Radiat.* **4**, 102 (1997).
- ²¹Y. Kubo and S. Asano, *Phys. Rev. B* **42**, 4431 (1990).
- ²²E. Zukowski, S. P. Collins, M. J. Cooper, D. N. Timms, F. Itoh, H. Sakurai, H. Kawata, Y. Tanaka, and A. Malinowski, *J. Phys.: Condens. Matter* **5**, 4077 (1993).
- ²³P. Fajardo, V. Honkimaki, P. Suortti, and Th. Buslaps (unpublished).
- ²⁴F. Biggs, L. B. Mendelsohn, and J. B. Mann, *At. Data Nucl. Data Tables* **16**, 201 (1975).
- ²⁵G. H. Lander, in *Handbook on the Physics and Chemistry of Rare Earths* (North-Holland, Amsterdam, 1993), Vol. 17, Chap. 117, p. 635.
- ²⁶B. D. Dunlap, I. Nowik, and P. M. Levy, *Phys. Rev. B* **7**, 4232 (1973).
- ²⁷Y. Berthier, R. A. B. Devine, and E. Belorizky, *Phys. Rev. B* **17**, 4137 (1978).